Genetic information transfer promotes cooperation in bacteria

Tatiana Dimitriu[a], Chantal Lotton[a], Julien Bénard-Capelle[a], Dusan Misevic[a], Sam P. Brown[b], Ariel B. Lindner[a,1], and François Taddei[a,1]

[a]Institut National de la Santé et de la Recherche Médicale U1001, Université Paris Descartes, Sorbonne Paris Cité, Faculté de Médecine Paris-Descartes, 75014 Paris, France; and [b]Centre for Immunity, Infection and Evolution, School of Biological Sciences, University of Edinburgh, Edinburgh EH9 3JT, United Kingdom

Edited by Bruce R. Levin, Emory University, Atlanta, GA, and approved June 17, 2014 (received for review April 18, 2014)

Many bacterial species are social, producing costly secreted "public good" molecules that enhance the growth of neighboring cells. The genes coding for these cooperative traits are often propagated via mobile genetic elements and can be virulence factors from a biomedical perspective. Here, we present an experimental framework that links genetic information exchange and the selection of cooperative traits. Using simulations and experiments based on a synthetic bacterial system to control public good secretion and plasmid conjugation, we demonstrate that horizontal gene transfer can favor cooperation. In a well-mixed environment, horizontal transfer brings a direct infectious advantage to any gene, regardless of its cooperation properties. However, in a structured population transfer selects specifically for cooperation by increasing the assortment among cooperative alleles. Conjugation allows cooperative alleles to overcome rarity thresholds and invade bacterial populations structured purely by stochastic dilution effects. Our results provide an explanation for the prevalence of cooperative genes on mobile elements, and suggest a previously unidentified benefit of horizontal gene transfer for bacteria.

bacterial cooperation | social evolution | plasmid transfer | gene mobility

Microorganisms produce a multitude of secreted factors, such as signaling, resource scavenging, virulence, or anticompetitor molecules (1). These so-called "public good" molecules are costly to produce but are accessible and potentially beneficial not just to the secreting organisms but to their neighbors as well. The production of the molecular public goods increases the fitness of neighboring individuals and can thus be considered as a cooperative behavior (2). The maintenance of cooperation is generally threatened by the spread of individuals that benefit from cooperation without paying the costs, so-called "nonproducers" or "cheaters." Social evolution theory predicts that cooperation can be maintained when its benefits are directed preferentially to organisms carrying cooperation genes. Several mechanisms that bias the partner association in cooperative interactions have been proposed (3, 4) and the recent application of sociobiology theories to microorganisms has opened them to experimental tests (5, 6). For example, limited dispersal of clone mates (7) or homophillic receptor binding (8) can generate a positive assortment among individuals carrying cooperative genes, which can be quantified by relatedness statistics (9). Assortment could additionally be modified at the gene level by the frequent and peculiar forms of sex in bacteria that make their genomes extremely plastic (10): genes often transfer within and between bacterial lineages, mainly by association with mobile genetic elements such as plasmids or phages (11). Strikingly, genes coding for cooperative traits, such as extracellular antibiotic degradation (12) or cholera toxicity (13), are often located on mobile elements (14, 15) suggesting a link between social behaviors and horizontal transfer.

Two mechanisms can explain the localization of cooperative genes on mobile elements. First, sufficiently high levels of horizontal transfer may promote mobile genetic elements purely as molecular parasites, despite their potential fitness cost to host cells (16). Mobility could then allow accessory genes to persist in the environment, even in the absence of continued positive selection (17). In the specific case of public good encoding genes, horizontal transfer of a cooperative producer allele could convert a recipient from nonproducer into a producer and thus enforce cooperation by infection (18). However, cooperation maintenance via infection enforcement is predicted to be unstable (14, 19), as a noncooperative allele will still displace a cooperative allele when both transfer horizontally. Second, horizontal transfer could modify the patterns of relatedness (gene assortment) in a population. Theoretical work suggests that horizontal gene transfer will increase relatedness at mobile loci, because the local spread of mobile alleles will increase the probability that neighboring individuals bear the same allele, favoring investment in cooperative traits at these loci (14, 20). However, experimental evidence that transfer can significantly modify the selective pressures acting on cooperative behaviors through either of these mechanisms is lacking. Here, for the first time to our knowledge, we experimentally investigate the effects of horizontal transfer on cooperation.

We developed a synthetic system in *Escherichia coli* with independent control of cooperation and conjugation. The cooperative trait is the secretion of a public good, namely the *Pseudomonas aeruginosa* quorum-sensing molecule C_4-HSL (21). The molecule is costly to produce but provides faster growth to both producer and nonproducer cells in the presence of the antibiotic chloramphenicol (Cm), by activating the expression of a chromosomal resistance gene. Using the conjugation machinery

Significance

Bacteria often cooperate through the production of public goods that change their environment. These processes can affect human health by increasing virulence or antibiotic resistance. Public good production is costly, making cooperation susceptible to invasion by nonproducing "cheater" individuals. Bacteria also readily share genes, even among distinct species. Our experiments and models converge to show that when both cheating and cooperative genes are transferred, cooperators win against cheaters because transfer increases assortment among alleles, favoring cooperation. This can explain why genes for cooperation are often mobile, and suggests that, in addition to reducing antibiotic resistance spread, preventing gene mobility could reduce cooperative virulence.

Author contributions: T.D., J.B.-C., A.B.L., and F.T. designed research; T.D. and C.L. performed research; T.D., C.L., J.B.-C., D.M., S.P.B., A.B.L., and F.T. analyzed data; and T.D., J.B.-C., D.M., S.P.B., A.B.L., and F.T. wrote the paper.

The authors declare no conflict of interest.

This article is a PNAS Direct Submission.

Freely available online through the PNAS open access option.

[1]To whom correspondence may be addressed. Email: ariel.lindner@inserm.fr or francois.taddei@inserm.fr.

This article contains supporting information online at www.pnas.org/lookup/suppl/doi:10.1073/pnas.1406840111/-/DCSupplemental.

of the F plasmid (22), we constructed a helper F plasmid which enables the transfer of the mobilizable (T^+) plasmids with (producer, P^+) or without (nonproducer, P^-) C_4-HSL public good gene, but does not transfer nonmobilizable (T^-) plasmids (Fig. 1*A*). Initial plasmid-free cells (recipients, R), P^+ and P^- plasmids are marked with distinguishable fluorescent proteins to enable monitoring of strain and plasmid dynamics using flow cytometry (Fig. 1*B* and Fig. S1). This synthetic approach allows us to study the effect of horizontal transfer in a biologically realistic setting without interference from plasmid–host coadaptation.

We implemented a simple metapopulation, consisting of subpopulations (demes) founded with different initial proportions of producers and nonproducers, and linked by migration (21) (Fig. 1*C* and *SI Text*). Previous work has shown that the higher growth rate of producer-rich populations in the presence of Cm can lead to a seemingly paradoxical statistical effect known as "Simpson's paradox" (21): although decreasing in proportion in individual populations, the overall number of producers across the metapopulation increases because producer-rich subpopulations have more individuals than producer-poor ones. In parallel, we built mathematical models parametrized using experimentally obtained values for the cost and benefit of public good production and cost and rates of transfer (*Materials and Methods* and *SI Text*). By numerically solving the models, we quantify cooperation dynamics in scenarios with different plasmid transfer rates within demes and migration rates among demes.

Results

Enforcement of Cooperation Is Unstable in a Well-Mixed Population. We first model (Fig. 2*A*) and test experimentally (Fig. 2*B*) the effect of horizontal transfer in a single well-mixed population where initially the majority of cells (97.5%) are recipients. In the absence of transfer (Fig. 2, blue), cooperation is not maintained. Producer plasmids pay the cost of public good production and are slightly outcompeted by nonproducer plasmids (3% decrease in P^+ ratio, $P = 0.02$). As expected (18), the transmissible producer plasmid (T^+P^+) outcompetes the nontransmissible nonproducer (T^-P^-) plasmid thanks to the invasion of recipients (23% increase in P^+ ratio, Fig. 2*B*, green; $P = 0.004$), leading to enforcement of cooperation because infectious transfer outweighs the cost of public good production for P^+-bearing cells. However, when P^- plasmids are transferable (T^+P^-), they outcompete both a nontransmissible P^+ plasmid (28% decrease in P^+ ratio, Fig. 2*B*, orange; $P = 5 \times 10^{-6}$) and a P^+ plasmid transferring at the same rate (7% decrease in P^+ ratio, Fig. 2*B*, red; $P = 3 \times 10^{-6}$). In the latter case, the benefit of transfer cancels out, and T^+P^- beats T^+P^+ by saving on production costs. Thus, as predicted by theory (19) and our models (Fig. 2*A*), transfer is not sufficient to maintain cooperation in a well-mixed population if both producer and nonproducer alleles are mobile.

Transfer Promotes Cooperation in a Structured Population. To study the competition between producer and nonproducer transmissible plasmids in a structured population, we implemented a simple metapopulation consisting of two subpopulations with different initial ratios of P^+ to P^- and identical proportions of plasmid-free recipients (Fig. 1*C*). The subpopulations grow separately in two distinct phases: transfer phase (no public goods benefit, no Cm, until t_1) and competition phase (public goods benefit, with Cm, from t_1 to t_2). At t_2 the two populations are mixed, mimicking a migration phase with global competition, and the relative success of the producer allele is measured as the change in P^+ proportion relative to P^-. In simulations, we also calculated an alternative metric, the absolute increase in P^+ proportion, including plasmid-free recipient cells (Fig. S2).

Our simulations predict that unlike in the single well-mixed population scenario, transmissibility of both P^+ and P^- plasmids does select for cooperation in a structured metapopulation, increasing the global proportion of P^+; cooperation is still disfavored when all plasmids are immobile (Fig. 3, *Inset* and Fig. S2). Our experiments confirm the result: producers are outcompeted in the absence of transfer (blue bar, Fig. 3, *Left*), but outcompete nonproducers when both plasmids can transfer (red bar, Fig. 3, *Left*). When the population is structured, transfer reverses the direction of the selective pressure and increases the global proportion of P^+ by 10% ($P = 6 \times 10^{-6}$).

The difference we observe can arise from either within- or among-population dynamics. Transfer does not increase the ratio of P^+ to P^- within each subpopulation (Fig. 3), as in the case of a well-mixed population. Thus, we can conclude that there is no direct infectious benefit of P^+ plasmids. However, the global P^+ proportion at the metapopulation level (Y_m) is disproportionally affected by within-population proportions (Y_1 and Y_2), based on each population's contribution to the total plasmid count. Let a be the bias in Y_m due to subpopulation growth differences. The effect of subpopulation size on Y_m can then be captured by the following relationship: $Y_m = [(1-a)Y_1 + (1+a)Y_2]/2$ (*SI Text*). In our experiments a increases with transfer from 0.08 to 0.37

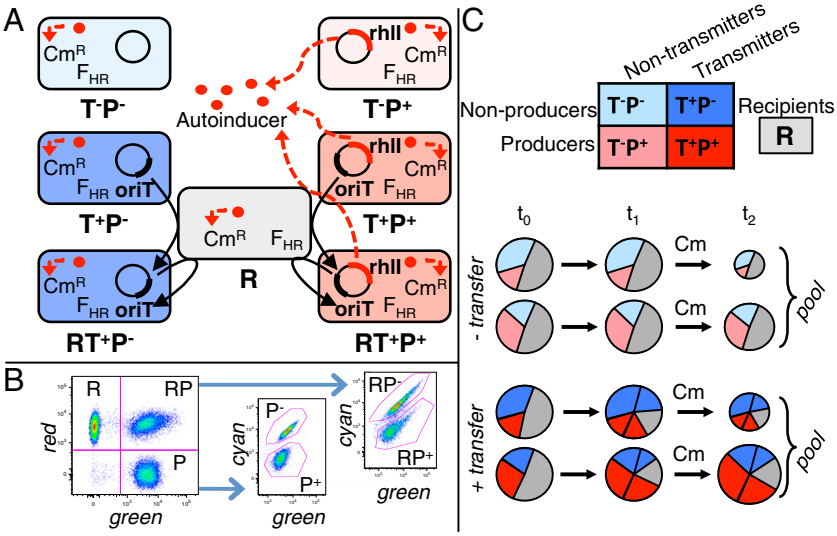

Fig. 1. Experimental system. (*A*) Synthetic system for conjugation and cooperation. P^+ cells express the synthase RhlI that produces C_4-HSL (RhI autoinducer, red dots), which diffuses (red arrows) and activates expression of Cm resistance (Cm^R) in all cells within a subpopulation. F_{HR} plasmid expresses F conjugation machinery and mobilizes plasmids bearing *oriT* (T^+) to recipient cells (black arrows), leading to RP^+ and RP^-, whereas plasmids without *oriT* (T^-) are not mobilized. (*B*) Flow cytometry. Recipients are marked with RFP, plasmids with YFP (P^+) or GFP (P^-). Initial plasmid bearers (P) and recipients without (R) or with (RP) plasmids are first distinguished with green and red filters, followed by separation of P^+ and P^- using green and cyan filters. (*C*) Experiment design. Public good producers (P^+, red) and nonproducers (P^-, blue) are mixed at t_0 with recipients (R) in subpopulations with varying ratios of P^+ to P^-. T^- plasmids (T^-P^+ and T^-P^-, pale colors) cannot be transmitted. T^+ plasmids (T^+P^+ and T^+P^-, bright colors) can be transmitted to recipients, yielding new plasmid bearers (respectively, P^+ and P^-). At t_1 subpopulations are diluted in medium containing Cm and grown until t_2, when they are pooled.

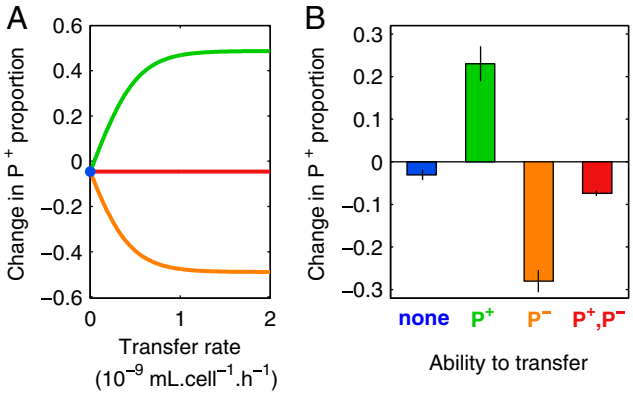

Fig. 2. Transfer favors producers as well as nonproducers in a well-mixed population. Initial proportions are 1.25% P^+, 1.25% P^-, and 97.5% R. The change in proportion of P^+ among all plasmids $P^+/(P^++P^-)$ is computed in the absence of public good benefits (no Cm, t_0 to t_1). (*A*) Simulated change in P^+ proportion as a function of transfer rate, given different population composition. Blue point represents the population with plasmids T^-P^- and T^-P^+ (no transfer), green line the population of T^-P^- and T^+P^+ (only P^+ transfer), orange line the population of T^+P^- and T^-P^+ (only P^- transfer), red line the population of T^+P^- and T^+P^+ (both P^- and P^+ transfer). (*B*) Experimental change in P^+ proportion in absence of transfer, or when one or both plasmids can transfer (color scheme the same as in *A*), shown as means ± SEM (n = 9). Statistically significant difference from zero was determined using a one-tailed t test.

($P = 4 \times 10^{-5}$), effectively amplifying Simpson's paradox and promoting cooperation. The effect is well captured by our simulations. In the presence of Cm, the subpopulation initially enriched in producer cells grows more rapidly than the other subpopulation (Fig. S3*A*). In the presence of transfer both populations grow more rapidly, but the size of the one with higher initial P^+ proportion increases more, exacerbating subpopulation size difference. Growth during the competition phase positively correlates with the amount of producers present after the transfer phase (Fig. S3*B*): the increase in population size differences is linked to an increased variation in P^+ abundance across populations, following plasmid transfer.

The effect of transfer on population genetic structure (due to both gene transfer and demographic effects) can be measured by relatedness. We calculate the producer relatedness (β^p_{Gg}; *Materials and Methods* and *SI Text*) following transfer, before cooperation becomes beneficial (at t_1; Fig. 1*C*). Transfer strongly increases relatedness in both simulations and experiments, but only for the mobile allele ($P = 0.004$, Fig. 4). The increase in relatedness is equivalent to an increase in the proportion of variance in producer frequencies among subpopulations (23, 24), which occurs because horizontal transfer spreads the cooperative allele locally, amplifying variations among subpopulations. To test if transfer acts on cooperation through its effect on assortment, we prevent it from increasing assortment in our simulations by implementing a global mixing of all transferred plasmids across populations after the transfer phase (Fig. S4, dashed line vs. plain line). Subsequently, P^+ proportion decreases despite no change in either costs or benefits of cooperation, or in the total rise in number of P^+ and P^- plasmids with transfer. Thus, our results indicate that transfer leads to a metapopulation-scale increase in cooperation via an increase in assortment among cooperators.

Transfer Effect on Cooperation Is Robust to Low Rates of Migration. Subpopulation differences supporting cooperation may be suppressed by migration, which homogenizes the genotype proportions across subpopulations. To investigate such a scenario, we introduce into our model an additional exchange of cells between subpopulations after transfer has occurred, but before subpopulations first encounter Cm (t_1; Fig. 1*C*). Both in the absence and presence of transfer, migration decreases the selection for P^+ (Fig. S5*A*), as it decreases the assortment among P^+ cells (Fig. S5*B*), and brings the metapopulation closer to a well-mixed population, partially avoiding the Simpson's paradox. For low rates of migration, transfer still promotes the selection of P^+. Horizontal transfer and migration have opposite effects on assortment, and sufficiently high migration effectively eliminates any increase in assortment due to transfer, highlighting that the effect of transfer is based on the existence of population structure. We should note that cooperation may still be maintained with high migration rates, if the mixing happens after the selection for cooperation has time to act (e.g., at t_2), exactly as we have implemented it in our experimental and modeling setup.

Cooperation Is Enhanced by Epidemic Spread Among Recipients. The effect of transfer relies on the presence of recipients and we expect that it will be affected by their abundance and properties. In our simulations, increasing the proportion of plasmid-free recipients decreases the strength of selection for producers in the absence of transfer (Fig. 5, black arrows). When producers are diluted by nonproducing cells, they benefit less from their own public good production and are therefore counterselected. Increased plasmid transfer (Fig. 5, red arrows) effectively opposes the producer scarcity by allowing plasmids to invade recipients, restoring selection of producers. The transfer-driven epidemic spread of producers has a stronger effect on producer proportion when the initial plasmid population is small and the number of plasmid-free recipients is high.

The plasmid epidemic also depends on the recipient's subsequent transfer ability. We simulate two extreme situations: (*i*) once infected, the recipients can also transfer plasmids (as is the case in our experiments), and (*ii*) recipients cannot transfer. Recipient transfer ability augments the effect of transfer on cooperator proportion (Fig. 5*A* vs. Fig. 5*B*) especially when the initial proportion of plasmids is low. Without secondary transfer,

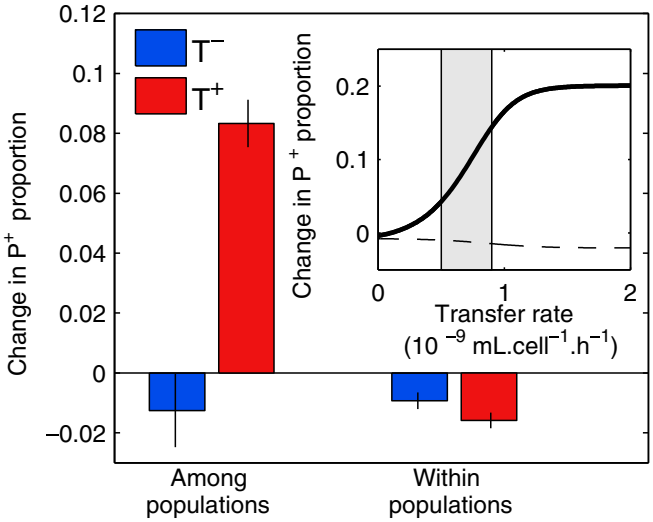

Fig. 3. Transfer selects for cooperation in structured populations. The metapopulation consists of two subpopulations, with 97.5% recipients and initial P^+/P^- ratios of 1:4 and 4:1. The change in proportion of P^+ among all plasmids $P^+/(P^++P^-)$ is computed during the competition phase (from t_1 to t_2, in the presence of Cm) without (blue) and with (red) transfer of both P^+ and P^- plasmids and shown as means ± SEM (n = 9). (*Inset*) Simulated change in P^+ proportion as a function of transfer rate, among (solid line) and within (dashed line) populations, the shaded area indicating estimated experimental transfer rates.

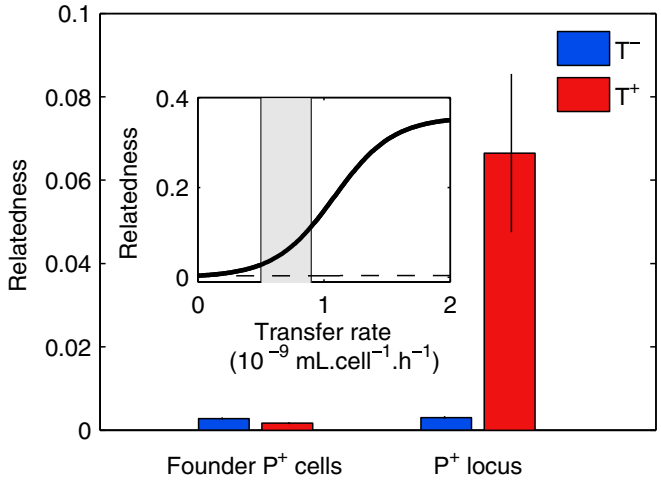

Fig. 4. Transfer selects for cooperation by increasing assortment among P^+ alleles. Parameters are the same as in Fig. 3. Assortment is evaluated by measuring relatedness, computed at t_1, without (blue columns) and with (red columns) transfer, shown as mean ± SEM ($n = 9$). Transfer significantly increases relatedness for the mobile allele (considering P^+ locus in all cells, $P = 0.004$) and slightly decreases relatedness for a nonmobile allele (considering only founder P^+ cells, $P = 0.005$). The decrease of relatedness considering only founder P^+ cells is due to a decrease in frequency of these cells during the transfer phase (t_0 to t_1) in the presence of transfer. (*Inset*) Simulated relatedness function of transfer rate for mobile (solid line) and nonmobile (dashed line) loci, the shaded area indicating estimated experimental transfer rates.

even at high transfer rates, the plasmids cannot spread fast enough to greatly modify the cooperative dynamics.

Transfer Can Promote Cooperation in Natural Scenarios. In our experiments, transfer does not create the initial variation, but only amplifies it. Variation in producer proportions could arise in nature when only a few plasmid-bearing cells colonize multiple populations of recipients. Because of the resulting low producer assortment among founder cells, we expect that the establishment of cooperation will depend on the presence of transfer. To simulate this scenario we implement strong dilutions leading to stochastic, Poisson-distributed number of founder cells (21). By varying both the founder cell dilution factor and the plasmid transfer rate we show that producers are selected only under strong dilution and high plasmid transfer conditions (Fig. 6). Weak dilution does not provide sufficient stochastic variation in the number of founder cells, and thus in producer proportions across populations, necessary for the rise in cooperation. Similarly, in the absence of transfer, the producers remain too rare to support cooperation. Transfer selects for cooperation by simultaneously amplifying the variation and overcoming the scarcity of cooperators created by the dilution. Notably, producer as well as nonproducer plasmids invade recipients thanks to horizontal transfer, but producers outcompete nonproducers thanks to their ability to exploit the increasing assortment, generating the Simpson's paradox.

Discussion

Through qualitative and quantitative agreement between experiments and simulations, we demonstrate the two previously suggested ways in which horizontal transfer can favor public good production. We first show that infectious transfer can increase cooperation in nonstructured populations (16, 18), but the effect is short-lived. Transfer directly benefits any allele, including nonproducer ones, which would take over the plasmid population (19). In contrast, we show that in structured populations, horizontal transfer specifically favors public good production by increasing the feedback of public goods benefits preferentially to producer alleles (14). This study thus provides, to our knowledge, the first experimental demonstration of the maintenance of a cooperative behavior through transfer of genetic information: plasmid conjugation modifies both allele frequencies and population structure enough to favor cooperation. Transfer and public good production interact in the way predicted by theory (18, 19), as confirmed by our experimental measurements and simulation tests of assortment, and with no interference from other biological processes. Our simulations further show that the effect of transfer in structured populations requires three conditions: variation in initial producer proportion, an abundance of plasmid-free cells, and low to intermediate migration during the transfer phase.

The assumptions about the population structure, composition, and dynamics we have made throughout our experiments and models are based on realistic real-world situations. For example, in our simulations, the initial stochastic variation in producer proportions arises through strong dilution. Consider the epidemic spread of a bacterial disease whose growth strongly depends on a bacterial public good (for instance a secreted toxin). In such a scenario, the founder variance would be repeatedly created when new hosts are infected by a low number of plasmid-bearing cells, and migration between hosts is likely to remain rare during infection. In each host, existing microbiome bacteria can act as recipients and amplify the production of the public good (25). Moreover, huge variability exists in plasmid presence and abundance across bacterial isolates (26). Naturally varying environments can change rapidly, altering plasmid costs and benefits (27), repeatedly leading to plasmid loss ensuring the formation of plasmid-free populations that will allow transfer to take place. Finally, our results rely on a sufficiently high transfer rate allowing plasmids to invade a significant part of a recipient population. The naturally observed rates are comparable (28), heterogeneous (29), and increased by mechanisms such as transient transfer derepression (30), leading to amplification of plasmid spread. Overall, we expect that the conditions for the dynamics we describe will be regularly encountered in nature.

In conclusion, our study shows that horizontal transfer can extend the parameter space where cooperation is favored, by both infectious propagation of cooperation and an increase in producer allele assortment. In our experimental setup, assortment is initially controlled by population structure, as the

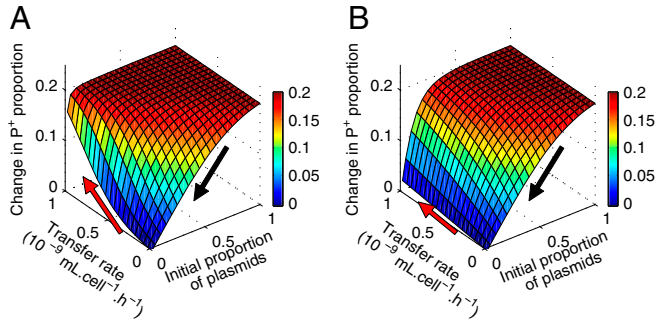

Fig. 5. Stronger transfer effect when recipients are abundant and amplify transfer. The metapopulation consists of two subpopulations, with initial P^+/P^- ratios of 1:4 and 4:1. Surfaces represent the change in proportion of P^+ among all plasmids, $P^+/(P^++P^-)$, during the competition phase (from t_1 to t_2, in the presence of Cm), as a function of transfer rate and initial proportion of plasmids in the population, $(P^++P^-)_{t0}$. (*A*) Change in P^+ proportion when recipients can also transfer plasmids. (*B*) Change in P^+ proportion when recipients cannot transfer plasmids. Black arrows indicate increasing proportion of plasmid-free cells, red arrows indicate increasing transfer rates.

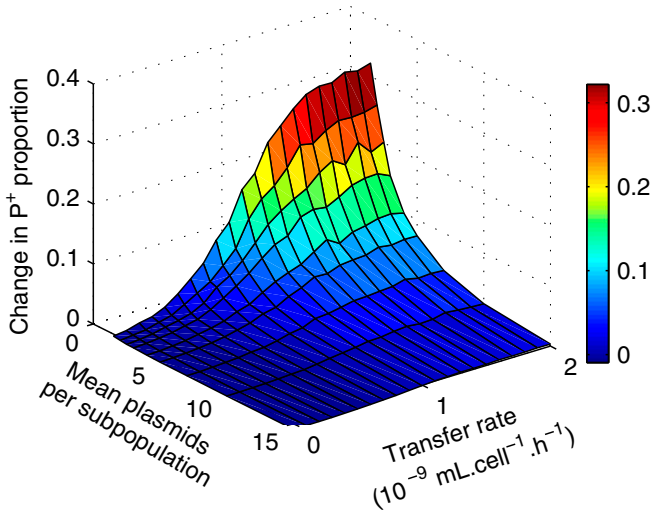

Fig. 6. Transfer allows rare producer genes to invade a bacterial metapopulation. The simulated metapopulation consists of 96 subpopulations initiated from a strongly diluted mix of (1%P^+, 1%P^-, 98%R), giving rise to Poisson distribution of P^+ and P^- across populations. The change of P^+ proportion among all plasmids, $P^+/(P^++P^-)$, during the competition phase (from t_1 to t_2, in the presence of Cm), is shown as a function of the transfer rate and the initial mean number of plasmid-bearing cells per subpopulation, averaged over 20 simulations.

probability of interactions between producer cells depends on their distribution among groups. Here we show that initially low relatedness is amplified by plasmid transfer, as suggested by theory (20). Horizontal transfer amplifies assortment because it acts at a local scale: conjugation requires cell contact and is thus necessarily local. Based on its effect on population structure, conjugation resembles other clustering mechanisms like multicellularity (31, 32), range expansion (33), budding dispersal (34), or group formation (35). However, it affects only specific genes carried on the infectious mobile genetic element, leading to different degrees of assortment for different genes from the same genome (36). We show experimentally that horizontal transfer strongly increases relatedness within a few generations because it is decoupled from and can happen faster than vertical transmission. Increasing relatedness at mobile loci (Fig. 4) improves the cost–benefit analysis for investment in the reproduction of neighboring cells (Fig. 3), as these cells are more likely to also carry cooperation genes due to infectious transfer. Gene assortment in the presence of mobile elements could be complicated by possible superinfections, where different competing plasmids inhabit the same cell (37), which would affect both the relatedness metric calculation and the cell phenotypes. However, superinfections are generally thought to be rare, due to widespread entry exclusion (38) and long-term segregation of incompatible plasmids (39). Our conclusions primarily concern the natural scenarios of epidemic spread in largely plasmid-free populations, rather than strong plasmid competition in nearly fully infected populations, where superinfection may evolve (37).

By demonstrating a link between infectious gene transfer (conjugation) and cooperation, our work has consequences for the understanding and management of bacterial communities. First, our results can explain the observed overrepresentation of cooperative genes (coding for secreted proteins) on mobile genetic elements (14, 15), as these genes will especially benefit from increased assortment. Additionally, mobile genetic elements are often associated with biofilm formation, another way of cell clustering that is physically induced by conjugation (40, 41). Biofilms could thus be another way for mobile elements to increase assortment which would not be gene-specific, but would still favor cooperation genes. Biofilms are themselves favorable to horizontal gene transfer (41), and could increase its gene-specific effect on relatedness. Second, our work suggests that by selecting for cooperation, horizontal transfer could provide adaptive benefits to host bacteria, shaped in turn by the degree of intragenomic conflict over directing benefits to neighboring cells (14). Plasmid-encoded cooperation may therefore modify selection for bacterial horizontal transfer mechanisms and contribute to the observed diversity in plasmid transfer rates among bacterial isolates (29). In bacteria, cooperation could represent an indirect selection pressure for sex, defined as any process selected by the benefits of genetic exchange (42), in addition to any direct advantage plasmids gain from transferring themselves. Finally, besides directly decreasing the spread of virulence and antibiotic resistance genes, targeting conjugation mechanisms (43) could hinder cooperative behaviors involved in the virulence of pathogenic bacteria by decreasing the range of conditions favoring the persistence of cooperative alleles.

Materials and Methods

Plasmids and Strains. The background strain is JC1191, an *E. coli* strain that can grow in low concentrations of Cm in the presence of C_4-HSL, thanks to the addition of *Pseudomonas* quorum sensing machinery (21). P^+ plasmid carries an artificial operon of yellow fluorescent protein (*YFP*) and *rhlI* under control of the strong promoter P_R. RhlI autoinducer synthase produces the Rhl autoinducer C_4-HSL (21). P^- plasmids carry green fluorescent protein (*GFP*) under control of P_R. Recipients bear pSB3K3-RFP plasmid expressing the *mRFP1* (red fluorescent protein) gene.

To provide transfer ability, cells bear the helper plasmid F_{HR}, a mutant of pOX38::Tc (44) with reduced mobilization efficiency by the F relaxase (1,000-fold reduction compared with F), and a deletion of the *traS* gene involved in entry exclusion. Recipient cells bearing F_{HR} are able to receive plasmids efficiently and behave as secondary donors. The F_{HR} plasmid provides efficient mobilization of T^+ plasmids present in the donor cell, which carry the wild-type origin of transfer *oriT* sequence of F plasmids, but no mobilization of T^- plasmids without *oriT*. Both P^+ and P^- plasmids have T^+ versions with *oriT*. Genotypes and relevant phenotypes of competitor plasmids are summarized in Fig. S1, and details about strains and plasmids are provided in *SI Text*.

Growth and Experiment Conditions. Details about the growth media are provided in *SI Text*. Experiments were conducted under well-mixed conditions. For the transfer phase of the experiments, strains were mixed at various ratios (vol/vol) and first grown from a 1:10 dilution (t_0; Fig. 1*C*) into medium lacking Cm, up to an optical density of 3. Strains were grown at 35 °C because F transfer is strongly reduced at 30 °C. When the initial proportion of P^+ and P^- plasmid-bearing cells was low, this step was repeated with maximum two successive dilutions into medium lacking Cm to increase plasmid transfer. Cultures were then diluted 1:10 and grown until stationary phase (t_1; Fig. 1*C*) at 30 °C, which allows preinduction of Cm resistance by C_4-HSL in nonproducer as well as producer cells and enhances the fluorescence signal. Finally, for experiments involving cooperation, cultures were diluted 1:100 into medium containing 6.25 μg/mL Cm (at t_1; Fig. 1*C*) and grown for 12–16 h at 30 °C until t_2 (Fig. 1*C*), where they were pooled. Cultures were analyzed for strain and plasmid proportions by flow cytometry (*SI Text*).

Relatedness. Relatedness $\beta_{G,g}$ quantifies genetic assortment by measuring how an individual's social environment *G* covaries with the individual's genotype *g*. Relatedness can be calculated as the linear regression coefficient connecting an individual's genotype (specifically, genetic value underlying the focal trait, here $g = 1$ if producer and 0 otherwise) with the genotype of its interactants (*G* is then the proportion of producers in the subpopulation of a focal individual) (9). Here, we focus on the relatedness of P^+, $\beta^P_{G,g}$, considering that the social environment of an individual corresponds to the local population it belongs to (see *SI Text* for details). Relatedness computed at the P^+ locus describes how much the benefits of public goods produced by P^+ will affect preferentially P^+-bearing cells because of population structure.

Model. We model the dynamics of producer (P^+) and nonproducer (P^-) alleles, carried on horizontally transmitted, incompatible plasmids (see *SI Text* for details). Plasmids can only be transferred to plasmid-free recipient cells (R). Producer cells (that bear P^+ plasmid) pay a cost of cooperation *c*. Transfer

follows a mass-action law (45): the number of transfer events is proportional to the product of plasmid-bearing (P^+ and P^-) and plasmid-free (R) cell densities in the local population. To mimic experimental conditions (growth limited by carrying capacity of the culture media), rates of transfer and growth follow a logistic function and decrease with the progressive consumption of resources until stationary phase at carrying capacity K. With the basal growth rate of ψ and basal rates of transfer of γ_{P^+} and γ_{P^-} for P^+ and P^-, respectively, the equations for growth and transfer are as follows:

$$\frac{dP^+}{dt} = [\psi(1-c) + \gamma_{P^+}R]P^+\left(1 - \frac{n_{tot}}{K}\right),$$

$$\frac{dP^-}{dt} = [\psi + \gamma_{P^-}R]P^-\left(1 - \frac{n_{tot}}{K}\right),$$

$$\frac{dR}{dt} = [\psi - (\gamma_{P^+}P^+ + \gamma_{P^-}P^-)]R\left(1 - \frac{n_{tot}}{K}\right).$$

We explicitly follow the experimental protocol by modeling the transfer and competition phases. From t_0 to t_1, preinduction of Cm resistance and transfer happen until stationary phase, without beneficial effects of public goods. From t_1 to t_2, the growth rate depends on the public good concentration, assumed to be proportional to the proportion of producing cells in the local population. For equations modeling initial and secondary plasmid bearers separately, Fig. 5*B*, see *SI Text*.

We model two types of metapopulations: a simple one with 2 separate subpopulations (all simulations except Figs. 2 and 6), and a metapopulation with 96 subpopulations arising from Poisson dilution of an initial cell mix (Fig. 6). Subpopulations grow separately until t_2, when they are pooled. For Figs. S4 and S5, we modeled additional migration between the two subpopulations at t_1 (see *SI Text* for details).

ACKNOWLEDGMENTS. We thank referees for comments; Antoine Frénoy, Jake Wintermute, Didier Mazel, and members of Institut National de la Santé et de la Recherche Médicale U1001 for advice and discussions; and Kevin Yauy for his contribution to pilot experiments. We also thank John Chuang for providing JC1191 strain and pZS*2R-GFP,rhlI plasmid, Didier Mazel for providing the pOX38::Tc plasmid, and the Cochin Cytometry and Immunobiology Facility for technical help. This work was supported by Agence Nationale de la Recherche "Evolution expérimentale de la coopération et du transfert d'informations" and "Who Am I?" Labex Sorbonne-Paris-Cité grants.

1. Crespi BJ (2001) The evolution of social behavior in microorganisms. *Trends Ecol Evol* 16(4):178–183.
2. West SA, Diggle SP, Buckling A, Gardner A, Griffin AS (2007) The social lives of microbes. *Annu Rev Ecol Evol Syst* 38(1):53–77.
3. Hamilton WD (1964) The genetical evolution of social behaviour. I. *J Theor Biol* 7(1): 1–16.
4. Frank SA (1998) *Foundations of Social Evolution* (Princeton Univ Press, Princeton).
5. Griffin AS, West SA, Buckling A (2004) Cooperation and competition in pathogenic bacteria. *Nature* 430(7003):1024–1027.
6. Gilbert OM, Foster KR, Mehdiabadi NJ, Strassmann JE, Queller DC (2007) High relatedness maintains multicellular cooperation in a social amoeba by controlling cheater mutants. *Proc Natl Acad Sci USA* 104(21):8913–8917.
7. Kümmerli R, Griffin AS, West SA, Buckling A, Harrison F (2009) Viscous medium promotes cooperation in the pathogenic bacterium *Pseudomonas aeruginosa*. *Proc Biol Sci* 276(1672):3531–3538.
8. Smukalla S, et al. (2008) FLO1 is a variable green beard gene that drives biofilm-like cooperation in budding yeast. *Cell* 135(4):726–737.
9. Gardner A, West SA, Wild G (2011) The genetical theory of kin selection. *J Evol Biol* 24(5):1020–1043.
10. Levin BR, Bergstrom CT (2000) Bacteria are different: observations, interpretations, speculations, and opinions about the mechanisms of adaptive evolution in prokaryotes. *Proc Natl Acad Sci USA* 97(13):6981–6985.
11. Thomas CM, Nielsen KM (2005) Mechanisms of, and barriers to, horizontal gene transfer between bacteria. *Nat Rev Microbiol* 3(9):711–721.
12. Lenski RE, Hattingh SE (1986) Coexistence of two competitors on one resource and one inhibitor: A chemostat model based on bacteria and antibiotics. *J Theor Biol* 122(1):83–93.
13. Waldor MK, Mekalanos JJ (1996) Lysogenic conversion by a filamentous phage encoding cholera toxin. *Science* 272(5270):1910–1914.
14. Nogueira T, et al. (2009) Horizontal gene transfer of the secretome drives the evolution of bacterial cooperation and virulence. *Curr Biol* 19(20):1683–1691.
15. Rankin DJ, Rocha EPC, Brown SP (2011) What traits are carried on mobile genetic elements, and why? *Heredity (Edinb)* 106(1):1–10.
16. Stewart FM, Levin BR (1977) The population biology of bacterial plasmids: A priori conditions for the existence of conjugationally transmitted factors. *Genetics* 87(2): 209–228.
17. Bergstrom CT, Lipsitch M, Levin BR (2000) Natural selection, infectious transfer and the existence conditions for bacterial plasmids. *Genetics* 155(4):1505–1519.
18. Smith J (2001) The social evolution of bacterial pathogenesis. *Proc Biol Sci* 268(1462): 61–69.
19. Mc Ginty SE, Rankin DJ, Brown SP (2011) Horizontal gene transfer and the evolution of bacterial cooperation. *Evolution* 65(1):21–32.
20. Mc Ginty SE, Lehmann L, Brown SP, Rankin DJ (2013) The interplay between relatedness and horizontal gene transfer drives the evolution of plasmid-carried public goods. *Proc Biol Sci* 280(1761):20130400.
21. Chuang JS, Rivoire O, Leibler S (2009) Simpson's paradox in a synthetic microbial system. *Science* 323(5911):272–275.
22. Frost LS, Ippen-Ihler K, Skurray RA (1994) Analysis of the sequence and gene products of the transfer region of the F sex factor. *Microbiol Rev* 58(2):162–210.
23. Pepper JW (2000) Relatedness in trait group models of social evolution. *J Theor Biol* 206(3):355–368.
24. Chuang JS, Rivoire O, Leibler S (2010) Cooperation and Hamilton's rule in a simple synthetic microbial system. *Mol Syst Biol* 6:398.
25. Stecher B, et al. (2012) Gut inflammation can boost horizontal gene transfer between pathogenic and commensal *Enterobacteriaceae*. *Proc Natl Acad Sci USA* 109(4): 1269–1274.
26. Boyd EF, Hill CW, Rich SM, Hartl DL (1996) Mosaic structure of plasmids from natural populations of *Escherichia coli*. *Genetics* 143(3):1091–1100.
27. Ellis RJ, Lilley AK, Lacey SJ, Murrell D, Godfray HCJ (2007) Frequency-dependent advantages of plasmid carriage by *Pseudomonas* in homogeneous and spatially structured environments. *ISME J* 1(1):92–95.
28. Simonsen L (1991) The existence conditions for bacterial plasmids: Theory and reality. *Microb Ecol* 22(1):187–205.
29. Dionisio F, Matic I, Radman M, Rodrigues OR, Taddei F (2002) Plasmids spread very fast in heterogeneous bacterial communities. *Genetics* 162(4):1525–1532.
30. Lundquist PD, Levin BR (1986) Transitory derepression and the maintenance of conjugative plasmids. *Genetics* 113(3):483–497.
31. Pfeiffer T, Bonhoeffer S (2003) An evolutionary scenario for the transition to undifferentiated multicellularity. *Proc Natl Acad Sci USA* 100(3):1095–1098.
32. Koschwanez JH, Foster KR, Murray AW (2011) Sucrose utilization in budding yeast as a model for the origin of undifferentiated multicellularity. *PLoS Biol* 9(8):e1001122.
33. Datta MS, Korolev KS, Cvijovic I, Dudley C, Gore J (2013) Range expansion promotes cooperation in an experimental microbial metapopulation. *Proc Natl Acad Sci USA* 110(18):7354–7359.
34. Kümmerli R, Gardner A, West SA, Griffin AS (2009) Limited dispersal, budding dispersal, and cooperation: an experimental study. *Evolution* 63(4):939–949.
35. Powers ST, Penn AS, Watson RA (2011) The concurrent evolution of cooperation and the population structures that support it. *Evolution* 65(6):1527–1543.
36. West SA, Griffin AS, Gardner A, Diggle SP (2006) Social evolution theory for microorganisms. *Nat Rev Microbiol* 4(8):597–607.
37. Smith J (2011) Superinfection drives virulence evolution in experimental populations of bacteria and plasmids. *Evolution* 65(3):831–841.
38. Garcillán-Barcia MP, de la Cruz F (2008) Why is entry exclusion an essential feature of conjugative plasmids? *Plasmid* 60(1):1–18.
39. Novick RP (1987) Plasmid incompatibility. *Microbiol Rev* 51(4):381–395.
40. Ghigo JM (2001) Natural conjugative plasmids induce bacterial biofilm development. *Nature* 412(6845):442–445.
41. Madsen JS, Burmølle M, Hansen LH, Sørensen SJ (2012) The interconnection between biofilm formation and horizontal gene transfer. *FEMS Immunol Med Microbiol* 65(2): 183–195.
42. Redfield RJ (2001) Do bacteria have sex? *Nat Rev Genet* 2(8):634–639.
43. Lujan SA, Guogas LM, Ragonese H, Matson SW, Redinbo MR (2007) Disrupting antibiotic resistance propagation by inhibiting the conjugative DNA relaxase. *Proc Natl Acad Sci USA* 104(30):12282–12287.
44. Anthony KG, Sherburne C, Sherburne R, Frost LS (1994) The role of the pilus in recipient cell recognition during bacterial conjugation mediated by F-like plasmids. *Mol Microbiol* 13(6):939–953.
45. Levin BR, Stewart FM, Rice VA (1979) The kinetics of conjugative plasmid transmission: Fit of a simple mass action model. *Plasmid* 2(2):247–260.

Supporting Information

Dimitriu et al. 10.1073/pnas.1406840111

SI Text

Plasmids and Strains. The background strain JC1191 (1) has the genotype *att::rhl-catLVA(Sp^R) ΔsdiA::FRT rrnB3 ΔlacZ4787 hsdR514 Δ (araBAD)567 Δ (rhaBAD)568 rph-1*. The att::rhl-catLVA(Sp^R) segment contains both an Rhl auto-inducer-responsive promoter (P_{rhl*}) driving an unstable version of *cat* [providing chloramphenicol (Cm) resistance], and the *rhlR* gene under the weak constitutive promoter P_{lacI}^q. This cassette is integrated into the chromosome with the spectinomycin resistance Sp^R. Therefore, the growth of JC1191 in Cm is strongly dependent on the Rhl autoinducer C_4-HSL: when present in sufficient concentration in the growth medium, C_4-HSL binds to the RhlR receptor and induces the expression of Cm resistance.

P^+ and P^- plasmids are low-copy plasmids with pSC101* replication origin. P^+ plasmid carries an artificial operon of *YFP* and *rhlI* (separated by a Shine–Dalgarno translation signal) under control of the strong promoter P_R. RhlI produces the Rhl autoinducer C_4-HSL (1). P^- plasmids carry *GFP* under control of P_R. P^+-bearing cells are public good producers, P^--bearing cells are nonproducers.

To provide transfer ability, all cells bear the helper plasmid F_{HR}. F_{HR} is a mutant of pOX38::Tc (2), where *oriT* contains two substitutions (A141T and C144G) that reduce binding and mobilization efficiency by the F relaxase compared with the wild-type F sequence (3). F_{HR} also bears a deletion of the *traS* gene: as TraS protein is responsible for the major part of entry exclusion of F plasmid (4), recipient cells bearing F_{HR} are able to receive T^+ plasmids efficiently, and behave as secondary donors. F_{HR} has strongly reduced self-transfer compared with F (1,000-fold reduction) but efficiently mobilizes *oriT*-bearing plasmids. The F_{HR} plasmid thus provides efficient mobilization of T^+ plasmids present in the cell, which carry the wild-type *oriT* sequence of F plasmids. Both P^+ and P^- plasmids have T^+ versions with *oriT*.

Recipients (R) bear pSB3K3-RFP, a medium-copy plasmid with p15A replication origin, carrying *mRFP1* under control of the strong promoter P_{lacI}. Recipients can receive T^+ plasmids (T^+P^+ and T^+P^- plasmids) but do not carry them initially: mRFP1 red fluorescence thus identifies recipient cells and secondary plasmid bearers brought by transfer from initial T^+-bearing cells to R cells.

P^+, P^-, and pSB3K3-RFP plasmids are maintained with kanamycin resistance genes.

Genotypes and relevant phenotypes of competitor plasmids and their identification by flow cytometry are summarized in Fig. S1.

Plasmids and Strains Construction. To construct P^+ plasmid used in our experiments, the YFP coding sequence (5) was amplified and cloned in pZS*2R-GFP,rhlI (1), replacing GFP. To construct P^- plasmid, pZS*2R-GFP,rhlI was digested with HindIII and XbaI and religated with the linker sequence AGCTTAATTAGCTGAGTCTAG to remove *rhlI*. T^+ plasmids were constructed by amplifying *oriT* from the F plasmid (coordinates 66002–66494 from GenBank NC_002483) and inserting it in the common SacI site of P^+ and P^- plasmids, in direct orientation. pSB3K3-RFP plasmid was obtained from the Registry of Standard Biological Parts (6).

F_{HR} plasmid was made in two steps. The first one was allelic exchange of pOX38::Tc (2) with a modified F *oriT* including mutations A141T and C144G, following the nomenclature in ref. 3. This mutated *oriT* was first cloned into the SacI site of pDS132 plasmid (7), then integrated in pOX38::Tc by allelic exchange with the wild-type sequence (7). In the second step, F_{HR} plasmid was obtained by deleting *traS* gene using λ/red homologous recombination (8): the sequence between F coordinates 88274 and 88606 was replaced by the *cat* cassette from pKD3, which was then removed with pCP20 (8). F_{HR} plasmid was transferred by conjugation to all strains needed, as it retains low conjugation ability.

Growth Conditions. Cells were grown in Luria-Bertani (BD Difco) medium with 25 μg/mL spectinomycin (Sp, Sigma-Aldrich) and 50 μg/mL kanamycin (Kn, Sigma-Aldrich), and with or without 6.25 μg/mL Cm (Sigma-Aldrich) and 0.75 μM C4-HSL. Experiments were conducted under well-mixed conditions with 5 mL medium in 50-mL tubes (Sarstedt).

For experiments involving public good benefits (all except Fig. 2), 0.75 μM C_4-HSL (CAS# 67605–85-0, Cayman Chemical) was added to the medium from the 30 °C-dilution step, as P^+ were found to outcompete P^- at low initial proportions, suggesting a differential benefit of low public good concentrations for producers; 0.75 μM C_4-HSL (mimicking the production of 2.5% P^+-bearing cells) restored the apparent cost of P^+, maintaining the configuration of the system in a state where cooperation is costly.

Note that markers are not stably maintained after transfer, as both T^+ and pSB3K3-P_{lacI}-RFP plasmids bear Kn-resistance markers, and one of the plasmids could be lost without the loss of resistance of the cell. However, this problem is minimized in our experimental setup: both types of plasmids are compatible, as they have different replication origins, and cells are cultured only for a short time period after the transfer actually happens. Despite potential for long-term marker loss, RFP fluorescence still accurately identifies cells on the timescale of our experiments. Indeed, we see no shift in the red fluorescence signal of transconjugants (that stays clearly distinct from the one of donor cells) compared with recipients during our experiments (Fig. 1*B*).

Flow Cytometry Analysis. Cultures were analyzed for strain and plasmid proportions by flow cytometry at t_0 and t_1 for experiments not involving public good benefits (Fig. 2), and at t_1 and t_2 for all other experiments. In the latter case, global proportions at the metapopulation scale were also measured by pooling equal volumes of each population.

For flow cytometry analysis of plasmid and strain proportions, cultures were fixed in 1% formaldehyde (Thermo Scientific) for 10 min, then resuspended in PBS (Life Technologies) and stored at 4 °C. Data acquisition was performed at the Cochin Cytometry and Immunobiology Facility. For each sample, 50,000 cells (increased to 100,000 cells when some competitors were present in proportions <1%) were analyzed using a LSRFortessa cell analyzer (BD Biosciences) with 405-, 488-, and 561-nm excitation lasers. Data analyses were performed using FlowJo (TreeStar). Recipients were identified with RFP, P^+ plasmids with YFP, and P^- plasmids with GFP fluorescence (Fig. S1). Cells with double RFP+YFP or RFP+GFP fluorescence were thus recipients that received, respectively, P^+ and P^-plasmids. After gating on forward and side scattering, three populations were first separated based on 530/30-nm and 670/30-nm filters (Fig. 1*C*, *Left*): P = (P^+, P^-), R and RP = (RP^+, RP^-). Then, P^+ and P^- cells in two of the populations were distinguished based on 530/30-nm and 525/50-nm filters, separating GFP and YFP (Fig. 1*C*, *Right*).

Whereas transfer can happen from T^+-plasmid-bearing cells to any of the cells present, our experimental setup ensured transfer would happen mainly to R cells. T^+-plasmid–bearing cells were

placed in very low initial proportions, making transfer to other T^+-bearing cells rare. Double GFP+YFP positive cells, arising either from transfer between T^+-bearing cells or from transfer of both P^+ and P^- plasmids to R cells, represented less than 2% of all cells analyzed and were excluded from the analysis.

Data Analysis. ***Selection of cooperation.*** As both plasmids increase in proportion with transfer, we estimate the relative success of the producer allele as P^+ change in proportion relatively to P^-, $P^+/(P^- + P^+)$ excluding recipients that do not bear P^+ or P^- plasmids. The global ratio at the metapopulation level was measured by pooling equal volumes of populations, effectively taking into account differential growth among populations. The mean ratio was computed as the mean of ratios within populations, to exclude this effect of differential growth.

We did not evaluate absolute changes experimentally, as optical density measurements evaluating absolute changes in cell density were found not to be accurate, potentially because of the aggregation of highly piliated cells, which may vary depending on the growth phases and experimental conditions.

To quantify the difference of within- and among-population ratios in a normalized way across experiments, we computed a coefficient a that represents how biased the global ratio is compared with a nonstandardized mean of populations (the bias arising from differential growth). Let Y_1 and Y_2 be, respectively, ratios in the producer-poor and producer-rich subpopulations, and Y_m the global ratio at the metapopulation level after mixing the two subpopulations. The coefficient a satisfies the equation $Y_m = [(1-a)Y_1 + (1+a)Y_2]/2$, and is thus defined as $a = (2Y_m - Y_1 - Y_2)/(Y_2 - Y_1)$.

Relatedness. In the main text we have already described the measure of genetic assortment, relatedness $\beta_{G,g}$. Here we provide a precise, numerical definition of the relatedness of P^+, $\beta^p_{G,g}$.

Let p_i and n_i be, respectively, the proportion of producers and number of bacteria within subpopulation i, and p_{tot} and n_{tot} be, respectively, the proportion of producers and number of bacteria in the metapopulation. Then, assuming populations are of the same size, which is the case at t_1, the relatedness of producers $\beta^p_{G,g}$ can be calculated as follows from the regression definition of relatedness (9):

$$\beta^p_{G,g} = \left(\sum_i \frac{p_i}{n_i} \frac{p_i}{p_{tot}} - \frac{p_{tot}}{n_{tot}} \right) \Big/ \left(1 - \frac{p_{tot}}{n_{tot}} \right).$$

To compute relatedness for nonmobile loci, we applied the same formula, but considering only P^+ alleles present in founder P^+ cells (i.e., excluding P^+ alleles present in recipient cells because of transfer).

Statistical analysis. Differences between conditions with and without transfer were tested with two-sample, two-sided t tests. The normality of distributions was confirmed with Shapiro–Wilkinson tests, rejecting the null hypothesis when $P < 0.05$. When normality was rejected, the nonparametric Wilcoxon signed-rank test was used instead of the t test.

Mathematical Modeling. ***Within-population dynamics.*** We model the dynamics of producer (P^+) and nonproducer (P^-) alleles, carried on horizontally transmitted, incompatible plasmids. Plasmids can be transferred to plasmid-free recipient cells (R) only, assuming entry exclusion between incompatible plasmids (10). Producer cells (that bear P^+ plasmid) pay a cost of cooperation c, nonproducers (P^- cells bearing P^- plasmid and plasmid-free R cells) do not. Transfer follows a mass-action law (11): the number of transfer events depends on the frequency of encounters between donor and recipient cells, assumed to be proportional to both donor cell (P^+ or P^-) and recipient cell (R) densities in the local population. The transfer rate constant γ (mL cell^{-1}·h^{-1}) describes the plasmid ability to transfer, and is expressed as the number of events per concentration (cell/mL), per unit time (h). Here, P^+ and P^- have transfer rates γ_{P+} and γ_{P-} respectively. We neglect plasmid loss, the effects of which are generally low compared with growth rate effects (12).

Growth follows a logistic function with cell densities saturating at a carrying capacity K, mimicking growth to stationary phase with the progressive consumption of resources (and neglecting cell death and turnover at this timescale of hours). We have chosen the specific mathematical form of our model to follow our experimental setup where cells grow in finite, exhaustible media (unlike a "chemostat" setting, often used for model simplification). If the population was then left in that state for a longer period, the individuals would start dying and a potentially more complex dynamic could develop over a much slower timescale. However, as our experiments are carried out in the timescale of hours, such long-term processes are not relevant.

Transfer saturates in the same way as growth, at carrying capacity K, as F transfer has been shown to strongly decrease when cells approach stationary phase (13).

The costs and benefits of public good production act solely on growth rate, as the public good does not liberate any additional resources and thus does not provide any enhancement to the carrying capacity. The carrying capacity is the same for all genotypes and is not affected by the presence of Cm (1) or the public goods (confirmed by experimental measurements for our modified strains, if the time of growth is extended beyond the one used in our experiments in the presence of Cm).

We explicitly follow the experimental setup by modeling its two steps. From t_0 to t_1, preinduction of Cm resistance and transfer happen until stationary phase similarly to experiments, without effects of public goods except their cost. The basal growth rate during this step is the constant rate ψ_1. From t_1 to t_2, the growth rate depends on the benefit of public goods b and on the public good concentration, assumed to be proportional to the proportion of producing cells in the local population P^+/n_{tot}. The basal growth rate during this step is ψ_2, which depends on the proportion of producers as follows: $\psi_2 = \psi_0 \times (1 + b \times P^+/n_{tot})$.

General equations for growth and transfer, which we present directly below, are common to the two steps (substituting, respectively, ψ_1 for ψ, from t_0 to t_1, and ψ_2 for ψ, from t_1 to t_2). We modeled two cases, with or without amplification of transfer by recipients that become secondary donors.

In the first case (all simulations except Fig. 5*B*), we model self-transfer of conjugative plasmids where conjugation controlling genes are also transferred (14), with amplification of transfer in recipients. This corresponds to the dynamics of plasmids in our experiments: with our experimental setup (Fig. 1*A*), conjugation genes from F_{HR} plasmid are not transferred but present in all cells, so conjugation is effectively controlled by *oriT* presence on transferred plasmids, making them similar to conjugative plasmids. Initial and secondary plasmid donors are not distinguished in the model.

$$\frac{dP^+}{dt} = [\psi(1-c) + \gamma_{P+}R]P^+\left(1 - \frac{n_{tot}}{K}\right),$$

$$\frac{dP^-}{dt} = [\psi + \gamma_{P-}R]P^-\left(1 - \frac{n_{tot}}{K}\right),$$

$$\frac{dR}{dt} = [\psi - (\gamma_{P+}P^+ + \gamma_{P-}P^-)]R\left(1 - \frac{n_{tot}}{K}\right).$$

In the second case (Fig. 5*B*), we assume that no secondary transfer happens from recipient cells. We thus model mobilization by factors present in the initial hosts, but not the secondary hosts (15). Initial plasmid bearers (I: IP^+ bearing P^+ plasmid and IP^-

bearing P^- plasmid) and recipients (noted R, RP^+, and RP^-, respectively, for plasmid-free, P^+-bearing, and P^--bearing recipient cells) are considered as separate genotypes, with $P^+ = IP^+ + RP^+$ and $P^- = IP^- + RP^-$:

$$\frac{dIP^+}{dt} = \psi(1-c)IP^+\left(1-\frac{n_{tot}}{K}\right),$$

$$\frac{dIP^-}{dt} = \psi IP^-\left(1-\frac{n_{tot}}{K}\right),$$

$$\frac{dR}{dt} = [\psi - (\gamma_{P+}IP^+ + \gamma_{P-}IP^-)]R\left(1-\frac{n_{tot}}{K}\right)$$

$$\frac{dRP^+}{dt} = [\psi(1-c)RP^+ + \gamma_{P+}IP^+R]\left(1-\frac{n_{tot}}{K}\right),$$

$$\frac{dRP^-}{dt} = (\psi RP^- + \gamma_{P-}IP^-R)\left(1-\frac{n_{tot}}{K}\right).$$

Metapopulation structure and selection. For the simulations presented in Fig. 2, the population is a well-mixed population.

We then model two types of metapopulations containing multiple separate populations.

For all other simulations except the one presented in Fig. 6, we model a simple metapopulation consisting of two separate populations that differ in their initial ratio of P^+ to P^- plasmids (t_0), and share the same proportion of R cells.

For simulations presented in Fig. 6, we model a metapopulation with 96 subpopulations where founder cells arise from a strongly diluted common mix of cells, giving rise to a Poisson distribution for each type of cell (1). This leads to stochastic variation in producer frequencies among subpopulations, and is generally similar to earlier models of cooperation via stochastic variation in compartmentalized populations (16).

Populations grow separately until t_2, where all populations are pooled. For Fig. S4, plasmid-bearing cells that arose from transfer (RP^+ and RP^-) were distributed in equal proportions in the two populations at t_1, keeping all other population parameters constant, and relatedness was computed after mixing. For Fig. S5, additional migration was modeled between the two populations at t_1 (after transfer): the migration rate is equal to the proportion of cells of each population that migrates to the other population at the t_1 time point.

To analyze the effect of pure infectious transfer (Fig. 2), changes in P^+ proportion were computed from t_0 to t_1 (as the public good benefits do not play a role in the infectious transfer hypothesis, and transfer happens efficiently from t_0 to t_1). When cooperation was involved (all other simulations), changes in P^+ proportion were computed from t_1 to t_2 (when public goods affect growth). As the public good acts on growth rate, the benefit of cooperation is only transient (1) and t_2 has to be chosen before all populations reach stationary phase. For each simulation, t_2 is defined as the time point where the selection of P^+ is maximal over all conditions tested.

Parameter values. Parameters values used in all models are shown below and were estimated from our experimental data:

Carrying capacity	$K = 4\times10^9$ cells mL^{-1}
Basal growth rate in the absence of Cm	$\psi_1 = 0.96\ h^{-1}$
Basal growth rate in the presence of Cm	$\psi_0 = 0.12\ h^{-1}$
Cost of public good production	$c = 0.04$
Benefit of cooperation on growth rate	$b = 4$.

The rates of transfer γ_{P+} and γ_{P-} were varied from 0 to 2×10^{-9} mL $cell^{-1}\cdot h^{-1}$, which encompasses the range of transfer rates that can be measured, and knowing that derepressed plasmids transfer at a rate around 10^{-9} mL $cell^{-1}\cdot h^{-1}$ (17). The rate was divided by 10 in the presence of Cm, to mimic experiments where growth in Cm happens at 30 °C and transfer is reduced. We did not attempt to measure γ experimentally, as the transfer rate is not constant during the duration of the experiments (because of successive dilutions and shifts in temperature). However, we can estimate an effective transfer rate that would lead to the plasmid invasion that was observed at t_1 in experiments. The measured effective transfer rates vary from 5×10^{-10} mL $cell^{-1}\cdot h^{-1}$ to 10^{-9} mL $cell^{-1}\cdot h^{-1}$ in our experiments.

The preincubation time was set to 12 h after 100-fold initial dilution from stationary phase cultures at carrying capacity, and growth in the presence of the antibiotic was allowed for 60 h after a second 100-fold dilution.

To study the effect of strong cell dilution (Fig. 6), cells were distributed in 96 populations each of 10 μL, following a Poisson distribution of parameter λ (P^+ and P^-) and 98 λ (R), ensuring an initial proportion of 2% plasmids. λ was varied from 1 to 15. Because of the strong initial dilution, the preincubation time was set at 24 h and a second 10-fold dilution step was added before t_1. Results were averaged over 20 replicate simulations, as strong variance arises from Poisson distribution.

All computer simulations were conducted using MATLAB.

1. Chuang JS, Rivoire O, Leibler S (2009) Simpson's paradox in a synthetic microbial system. *Science* 323(5911):272–275.
2. Anthony KG, Sherburne C, Sherburne R, Frost LS (1994) The role of the pilus in recipient cell recognition during bacterial conjugation mediated by F-like plasmids. *Mol Microbiol* 13(6):939–953.
3. Stern JC, Schildbach JF (2001) DNA recognition by F factor TraI36: highly sequence-specific binding of single-stranded DNA. *Biochemistry* 40(38):11586–11595.
4. Achtman M, Kennedy N, Skurray R (1977) Cell—cell interactions in conjugating *Escherichia coli*: role of traT protein in surface exclusion. *Proc Natl Acad Sci USA* 74(11):5104–5108.
5. Elowitz MB, Levine AJ, Siggia ED, Swain PS (2002) Stochastic gene expression in a single cell. *Science* 297(5584):1183–1186.
6. Registry of Standard Biological Parts http://parts.igem.org/.
7. Philippe N, Alcaraz J-P, Coursange E, Geiselmann J, Schneider D (2004) Improvement of pCVD442, a suicide plasmid for gene allele exchange in bacteria. *Plasmid* 51(3):246–255.
8. Datsenko KA, Wanner BL (2000) One-step inactivation of chromosomal genes in *Escherichia coli* K-12 using PCR products. *Proc Natl Acad Sci USA* 97(12):6640–6645.
9. Gardner A, West SA, Wild G (2011) The genetical theory of kin selection. *J Evol Biol* 24(5):1020–1043.
10. Garcillán-Barcia MP, de la Cruz F (2008) Why is entry exclusion an essential feature of conjugative plasmids? *Plasmid* 60(1):1–18.
11. Levin BR, Stewart FM, Rice VA (1979) The kinetics of conjugative plasmid transmission: fit of a simple mass action model. *Plasmid* 2(2):247–260.
12. Lau BTC, Malkus P, Paulsson J (2013) New quantitative methods for measuring plasmid loss rates reveal unexpected stability. *Plasmid* 70(3):353–361.
13. Frost LS, Manchak J (1998) F- phenocopies: Characterization of expression of the F transfer region in stationary phase. *Microbiology* 144(Pt 9):2579–2587.
14. Stewart FM, Levin BR (1977) The population biology of bacterial plasmids: A priori conditions for the existence of conjugationally transmitted factors. *Genetics* 87(2):209–228.
15. Levin BR, Stewart FM (1980) The population biology of bacterial plasmids: A priori conditions for the existence of mobilizable nonconjugative factors. *Genetics* 94(2):425–443.
16. Szathmáry E, Demeter L (1987) Group selection of early replicators and the origin of life. *J Theor Biol* 128(4):463–486.
17. Simonsen L (1991) The existence conditions for bacterial plasmids: Theory and reality. *Microb Ecol* 22(1):187–205.

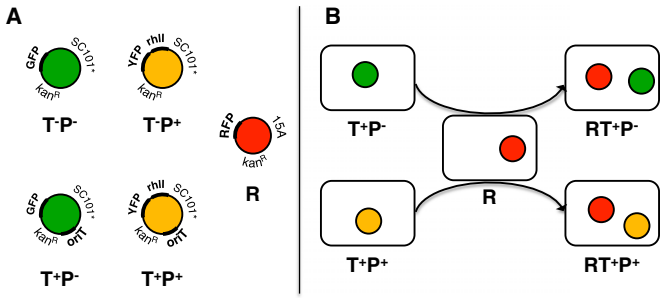

Fig. S1. Plasmids used in experiments and strain identification. Plasmids are colored according to the fluorescence genes they bear. (*A*) Plasmids used in experiments. pSC101-origin (pSC101*) bearing plasmids are responsible for transfer and production phenotypes. P^- and P^+ indicate public good production status: P^+ plasmids express RhlI synthase and YFP; P^- plasmids express only GFP. T^- and T^+ indicate transfer status, T^+ are transferable as they bear F *oriT*. Recipients bear a compatible plasmid (with p15A replication origin) expressing RFP. p15A-origin and pSC101-origin bearing plasmids all bear a kanamycin resistance gene (kan^R). (*B*) Identification of strains and plasmids with plasmid fluorescence genes. Initial strains are marked with only one fluorescence plasmid (the case of T^+ plasmids is represented here). With transfer, recipients bearing two plasmids arise, and are identified by the combination of RFP and GFP or RFP and YFP fluorescence.

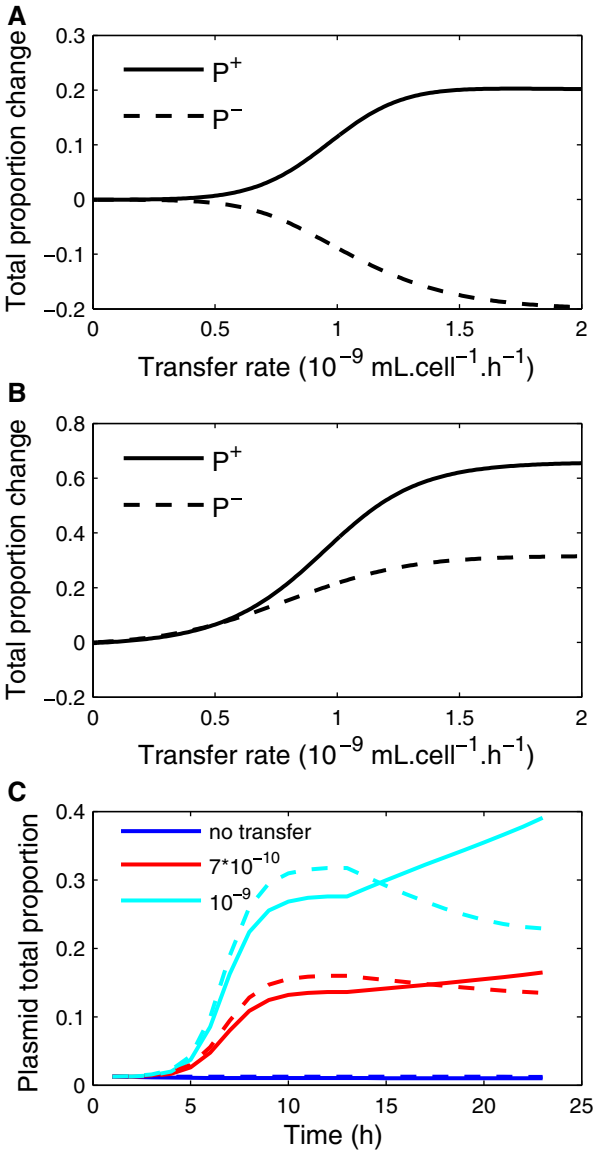

Fig. S2. Dynamics of plasmids in the total metapopulation. The metapopulation is the same as in Fig. 3. The changes in proportion of P^+ and P^- in the total population [respectively, $P^+/(P^++P^-+R)$, plain lines, and $P^-/(P^++P^-+R)$, dashed lines] are computed in simulations from t_1 to t_2 (*A*) and from t_0 to t_2 (*B*) as a function of the common transfer rate of P^+ and P^-. Infectious transfer takes place mainly from t_0 to t_1; public goods affect population growth from t_1 to t_2. As an example, plasmid proportions are also shown as a function of time (*C*) in the absence of transfer (blue), for a transfer rate of 7×10^{-10} mL $cell^{-1} \cdot h^{-1}$ (that corresponds to the estimated experimental transfer rate, red) and a transfer rate of 10^{-9} mL $cell^{-1} \cdot h^{-1}$ (cyan).

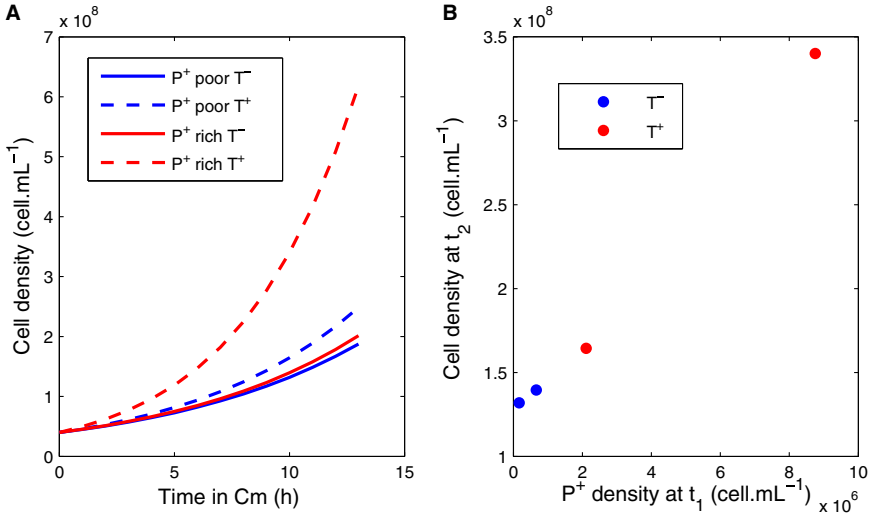

Fig. S3. Growth of subpopulations in the presence of Cm. The total cell density is computed in simulations for P^+-poor (blue) and P^+-rich (red) populations, in the absence (T^-) or presence (T^+) of transfer at a rate of 7×10^{-10} mL cell^{-1}·h^{-1} (that corresponds to the estimated experimental transfer rate). Parameters are the same as in Fig. 3. In *A*, the total density is shown as a function of time in the presence of Cm (from t_1 to t_2). In *B*, the total density is shown at t_2 as a function of P^+ density at t_1 (after most of the transfer happened).

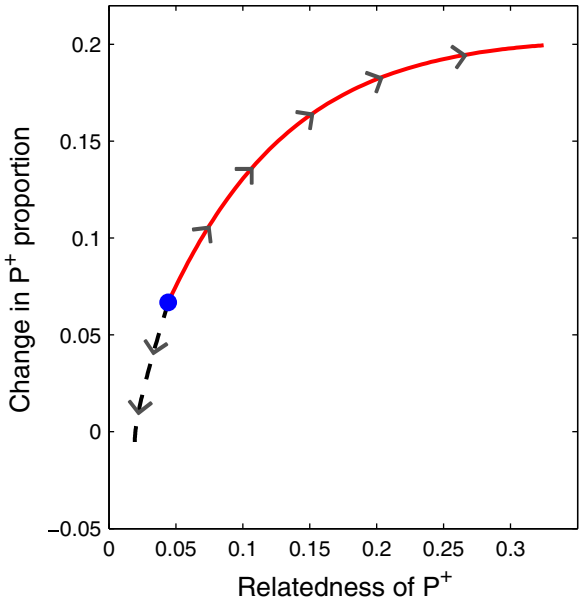

Fig. S4. Transfer selects for cooperation by increasing assortment among P^+ alleles. Parameters are the same as in Fig. 3, except recipient's proportion, which is 75%. The simulated change in P^+ proportion is shown as a function of P^+ relatedness, with transfer within populations (solid red line) or randomized across populations (dashed black line). Arrows indicate the direction of increasing transfer rates, the blue dot indicating absence of transfer.

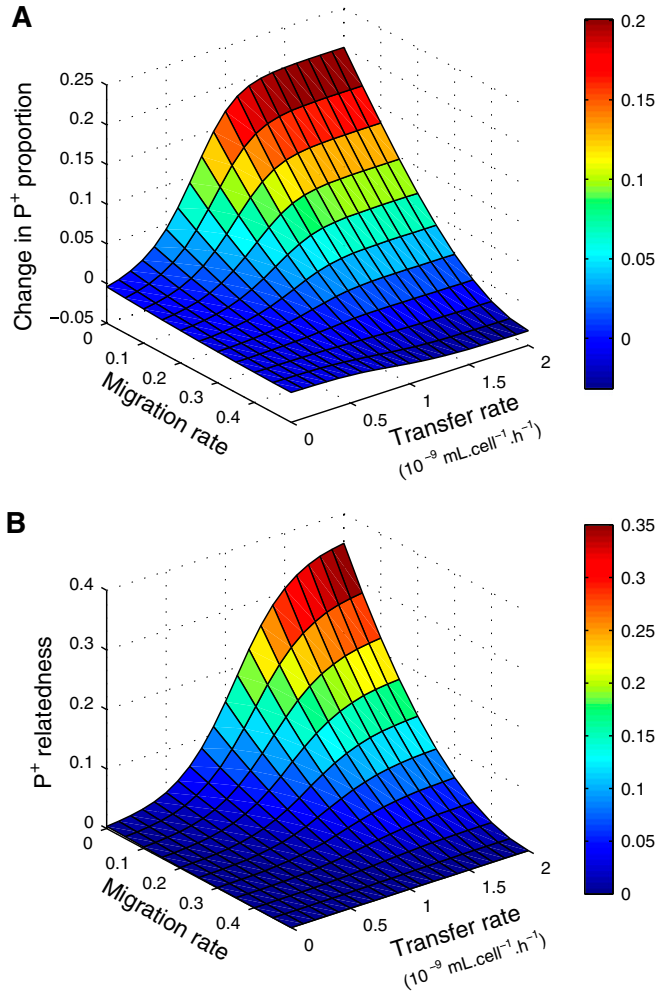

Fig. S5. Transfer and migration have antagonistic effects on the selection of cooperation. The metapopulation consists of two subpopulations, with initial P^+/P^- ratio of 1:4 and 4:1. The surface represents the change in proportion of P^+ among all plasmids $P^+/(P^++P^-)$ in the presence of Cm (from t_1 to t_2) (*A*) and P^+ relatedness at t_1 (*B*), as a function of the common transfer rate of P^+ and P^- plasmids and of the migration rate between the two populations (proportion of cells that are exchanged between the two populations at t_1).